Society For Biomaterials

Damage mechanisms at the cement–implant interface of polished cemented femoral stems

AQ6 Natalie Shearwood-Porter,[1] Martin Browne,[1] James A. Milton,[2] Matthew J. Cooper,[2] Martin R. Palmer,[2] Jeremy M. Latham,[3] Robert J. K. Wood,[4] Richard B. Cook[4]

AQ2 [1]Bioengineering Science Research Group, University of Southampton, Southampton, UK
[2]School of Ocean and Earth Science, University of Southampton, National Oceanography Centre, Southampton, UK
[3]Southampton Orthopaedic Centre for Arthroplasty and Revision Surgery (SOCARS), Southampton General Hospital, Southampton, UK
[4]National Centre for Advanced Tribology at Southampton (nCATS), University of Southampton, Highfield, Southampton, UK

Received 9 November 2015; revised 10 May 2016; accepted 6 June 2016
Published online 00 Month 2016 in Wiley Online Library (wileyonlinelibrary.com). DOI: 10.1002/jbm.b.33739

Abstract: The occurrence of damage on polished femoral stems has been widely reported in the literature, and bone cement has been implicated in a tribocorrosive failure process. However, the mechanisms of cement-mediated damage and the impact of cement formulation on this process are not well understood. In this study, 13 Zimmer CPT polished femoral stems, and the corresponding cement specimens were retrieved at revision surgery and analyzed using high-resolution imaging techniques. Surface damage attributed to tribocorrosion was observed on all stems. Corrosion product, in the form of black flaky surface debris, was observed on the surface of cement specimens; both energy-dispersive X-ray spectroscopy and inductively coupled plasma mass spectrometry(ICP-MS) confirmed the presence of cobalt and chromium, with the ICP-MS showing much higher levels of Cr compared to Co when compared to the original stem material. Agglomerates of ZrO_2 radiopacifier were also identified on the cement surface and, in some cases, showed evidence of abrasive wear; the size of these particles correlated well with elliptical pitting evident on the surfaces of the corresponding stems. This evidence supports the hypothesis that agglomerates of hard radiopacifier particles within the cement may induce a wear-dominated tribocorrosive interaction at the stem–cement interface that damages the surface of polished CoCr femoral stems. © 2016 Wiley Periodicals, Inc. J Biomed Mater Res Part B: Appl Biomater 00B: 000–000, 2016.

Key Words: bone cement, implant retrieval, failure analysis, cobalt–chromium alloys, corrosion

How to cite this article: Shearwood-Porter N, Browne M, Milton JA, Cooper MJ, Palmer MR, Latham JM, Wood RJK, Cook RB. 2016. Damage mechanisms at the cement–implant interface of polished cemented femoral stems. J Biomed Mater Res Part B 2016:00B:000–000.

INTRODUCTION

Damage to the surfaces of cemented femoral stems has been reported in a number of retrieval studies involving a range of stem designs and cement formulations.[1–6] The damage has been attributed to abrasion,[7] metallic shedding,[8,9] tribocorrosion,[4,10,11] originating from micromotion between the stem and cement mantle,[12] pores at the cement surface,[13] the radiopacifier, and the cement chemistry,[10,14,15] with the stem design, cement formulation, and location on the stem affecting the damage mechanisms.[16,17]

A great deal of work has been undertaken by Bryant et al.[4,11,14,15,18] to identify the origins and drivers of damage, and this has led to the proposal of a fretting-corrosion mechanism.[18] The mechanism describes how the oxide film on the surface of the CoCrMo stem and bone cement are in intimate contact when the stem is inserted. When loaded during the stance phase of the gait cycle, the contact pressures on the asperities of the two surfaces exceed the yield stress of the oxide film, bone cement, and CoCrMo stem, causing oxide film fracture, transfer of the oxide to the cement surface, and plastic deformation of the cement and stem surfaces. During the swing phase of the gait cycle, the interface separates, exposing the depassivated metal surface to the body fluids enabling dissolution of the metal and the oxide film to reform. The repetition of this process results in a build-up of damage on the stem surface and an accumulation of the fractured oxide film between the cement and the stem surfaces, seen as black deposits and flakes on the stem and cement surfaces. This mechanism provides an explanation for the origins of the Cr_2O_3 film. However, the detailed analysis focused on the tribofilm and surface of the stem with no review of the cement surface, and the mechanism stops short of explaining how the comparatively soft PMMA bone cement (0.32

AQ3 **Correspondence to**: R. B. Cook; e-mail: r.b.cook@soton.ac.uk
Contract grant sponsor: EPSRC through the Green Tribology Platform grant (Natalie Shearwood-Porter); contract grant number: EP/J001023/1

GPa) can plough and plastically deform the surface of a hard CoCrMo alloy (6.0 GPa[19]).

The aim of this study was to conduct a detailed forensic examination of a selection of femoral stems and the corresponding proximal cement mantles of failed large diameter MOM THA, in order to investigate cement-mediated damage mechanisms at the cement–implant interface of polished femoral components.

MATERIALS AND METHODS

Twelve Zimmer CPT polished, collarless tapered cobalt-chrome femoral stems, implanted between 2002 and 2007, were retrieved during revision surgery. The implants were hybrid modular THA with cemented femoral components, both from mixed and matched manufacturer stem and head combinations, as described previously by Ref. 5. Indications for revision included adverse local tissue reactions aseptic loosening, pain, and raised serum concentration of cobalt (Co) and chromium (Cr) ions. Time *in vivo* ranged from 52 to 97 months. Detailed characteristics for each retrieved
T1 femoral stem are given in Table I.

Fragments of acrylic bone cement were retrieved for eight stems. Cement was collected from the proximal region of the cement mantle (corresponding to Gruen zones 1 and 7) and was associated with both macroscopically damaged and undamaged surfaces of the stem; to avoid artefacts arising from instrument damage, only cement that was easily removed was included in the study. In the cases of high levels of damage, the cement surfaces were covered with a layer of black deposit. In each case, the retrieved cement was either vacuum-mixed Palacos R40G (Schering Plough, Welwyn Garden City, UK) or Biomet Palacos (Biomet UK, Bridgend, UK); these are poly(methylmethacrylate/methylacrylate) (PMMA)-based formulations containing ∼15% (w/w) zirconium dioxide (ZrO_2) radiopacifier and a variable amount of gentamicin sulphate in the powder component(-depending on the manufacturer).

Femoral stems were imaged using an Alicona InfiniteFocus microscope (Alicona Imaging GmbH, Graz, Austria). The technique uses optical microscopy and focus variation technology to extract three-dimensional morphology and depth information from the surface with a resolution of 10 nm.

Cement fragments were imaged using a JEOL JSM6500F field emission gun scanning electron microscope (SEM) (JEOL USA, Peabody, MA). Specimens were sputter-coated with a thin layer (∼15 nm) of gold prior to imaging. A low accelerating voltage (5–10 kV) was employed in order to minimise artefacts arising from beam-induced polymer degradation, and imaging at very high magnifications (>5000×) was interpreted with caution. Elemental analysis of the surface of the cement specimens was conducted using energy-dispersive X-ray spectroscopy (EDX).

A sample of the black deposit on the surface of one of the cement samples was removed using tweezers. The sample was weighed in a Teflon digestion vessel and subjected to a sequential digestion in concentrated HCl at 130°C overnight, followed by a concentrated HNO_3/HF at 130°C

TABLE I. Patient and Implant Characteristics

Number	Femoral Head	Patient Age at Primary	Patient Gender	Indication for Primary	Time *In Vivo* (Months)	Indication for Revision	Stem Loose at Revision?	Cement Obtained?	Blood Co (nmol/L)	Blood Cr (nmol/L)
1	BHR	64	M	OA	56	Aseptic loosening, lesser troch fracture	Yes	No	159	111
2	BHR	70	M	OA	86	Aseptic loosening, raised metal ions	Yes	No	177	129
3	BHR	44	F	Dysplasia	80+	Pain + raised metal ions	No	Yes	61	23
4	BHR	68	F	OA, dysplasia	85	Pain + raised metal ions	Yes	Yes	218	191
5	BHR	68	M	OA	89	Pain + raised metal ions	No	No	168	66
6	Adept	57	F	OA, dysplasia	52	Pain + raised metal ions	No	No	72	113
7	Adept	60	M	AVN	81	Pain + raised metal ions	Yes	Yes	191	256
8	BHR	74	F	OA	94	Pain + recurrent troch bursitis	No	Yes	79	40
9	BHR	56	F	OA	97	Pain + raised metal ions	No	Yes	185	151
10	BHR	59	F	Unknown	96	Pain	No	Yes	159	111
11	BHR	79	F	Unknown	88	Pain + raised metal ions	Yes	Yes	177	129
12	BHR	69	F	Unknown	69	Pain	No	Yes	70	32

COLOR

FIGURE 1. Photographs of the posterior and medial views of two stems demonstrating the variation in severity of damage to the stem surfaces.

overnight and finally an Aqua Regia digest at 130°C overnight. Despite this aggressive digestion, a small amount of solid dark residue remained in the base of the digestion vessel. This residue was investigated using EDX and shown to contain Cr and Fe (although the amount of material was too low and too fine-grained to obtain quantitative data). The dissolved samples were then evaporated to dryness and redissolved in 3% HNO_3 spiked with 20 ppb of Be and 5 ppb of In and Re to act as internal standards. Mass spectroscopy was carried out using a X-SERIES 2 ICP-MS (Thermo Fisher Scientific, Bremen, Germany). Data were acquired for all isotopes of interest in peak-jumping mode (4 $\times$ 30 second repeats per sample). After each sample analysis, a wash solution containing 3% HNO_3 was run until background levels were achieved. The raw data were blanked and internally corrected and then calibrated against synthetic standards (Inorganic Ventures, Virginia).

RESULTS

Stem surface

The location and severity of damage varied between stems. All stems showed evidence of macroscopic material loss on the posteromedial aspect, ranging from one or two isolated spots a few millimeters in diameter to extensive patches extending to the under neck region, as shown in Figure 1 F1 Damaged regions were also frequently observed on the anterolateral regions of the stems and occasionally on the anterior face. Surface deposits, in the form of black or brown plaques, were also noted.

Microscopically, the appearance of damaged regions at the proximal end of the cement stem interface was indicative of fretting corrosion (Figure 2). Extensive deformation F2 and damage of the stem surface was noted, with "islands" of apparently undamaged material. Damaged regions occurring on the medial side of the posterior surface frequently demonstrated a unidirectional alignment, $\sim$45° to the long axis of the stem (Figure 2).

Cement surface

Fragments of the full thickness cement mantle were obtained. The surface of the cement in contact with the stem was easily identified by the presence of a typically smooth, uniformly flat or curved surface [Figure 3(a)] and/ F3 or black deposits with a flaky appearance [Figure 3(b)]. The green colouring of the cement is consistent with the formulation of Palacos R + G due to the addition of chlorophyll.

Examination of bone cement fragments using SEM demonstrated differing degrees of damage at the cement surface according to the region of contact with the stem. Agglomerates of zirconium dioxide (ZrO_2) particles, typically 5 μm in diameter and with a cauliflower-like appearance, were visible within the cement; the identity of these agglomerates was verified using EDX. The undamaged regions showed evidence of micropores at the surface of the cement (Figure 4). EDX within the F4 pores showed evidence of $Zr0_2$ particles (Figure 4).

On the moderately damaged regions of the cement (Figure 5), both radiopacifier and metallic debris were identi- F5 fied via EDX. Although traces of Co and Mo were noted, Cr was found to be the dominant metallic species. Inspection

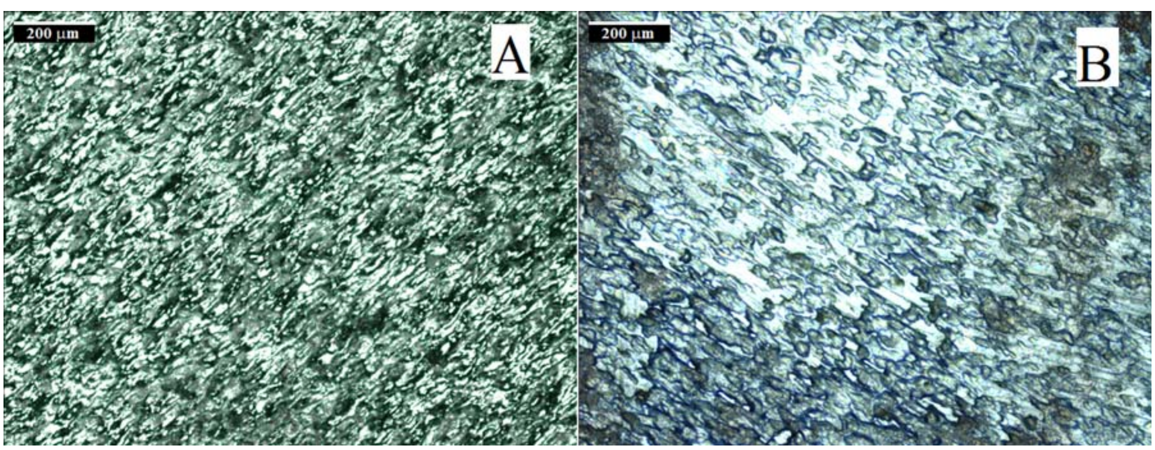

COLOR

FIGURE 2. Optical micrographs of damage to stem 4 (A) and stem 8 (B) surface showing directionality to the proximal surface damage.

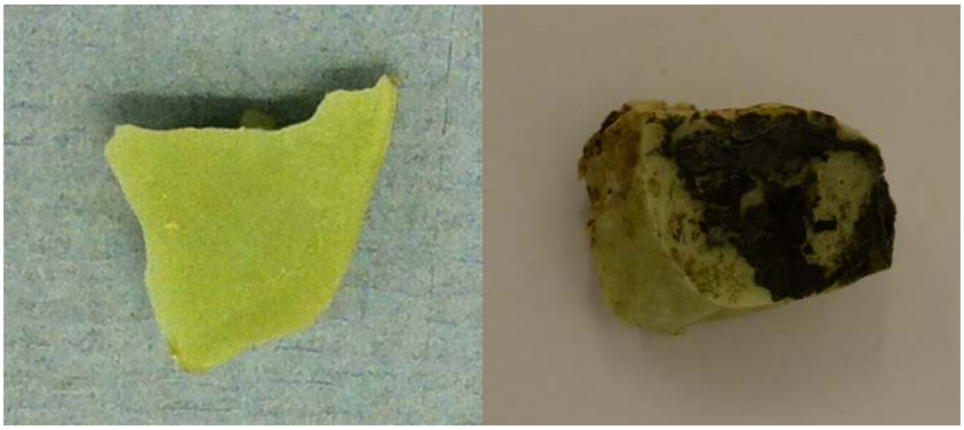

COLOR

FIGURE 3. (a) Cement fragment from a region of low cement and stem damage showing a smooth and uniformly flat surface. (b) Cement fragment from a high damage region with corrosion product visible on the surface of the cement.

of the highly damaged regions showed the ZrO_2 agglomerates standing proud from the underlying cement [Figure F6 6(a,b)], with the surfaces of the agglomerates flattened [Figure 6(c,d)]; the cement also appeared to have been abraded, with evidence of directional wear [Figure 6(a)].

The sample of corrosion product analyzed by ICP-MS identified a number of metallic elements within the corrosion product (Table II.IC). T2 Comparison of the three main elemental constituents of the stem, that is, Cr, Co, and Mo, revealed a very high concentration of Cr in the corrosion product, 10 times greater than the concentration of Co, while the Mo concentration was found to be negligible.

DISCUSSION

This study is the first to review the surface of retrieved bone cement from THRs and relate it to the damage seen

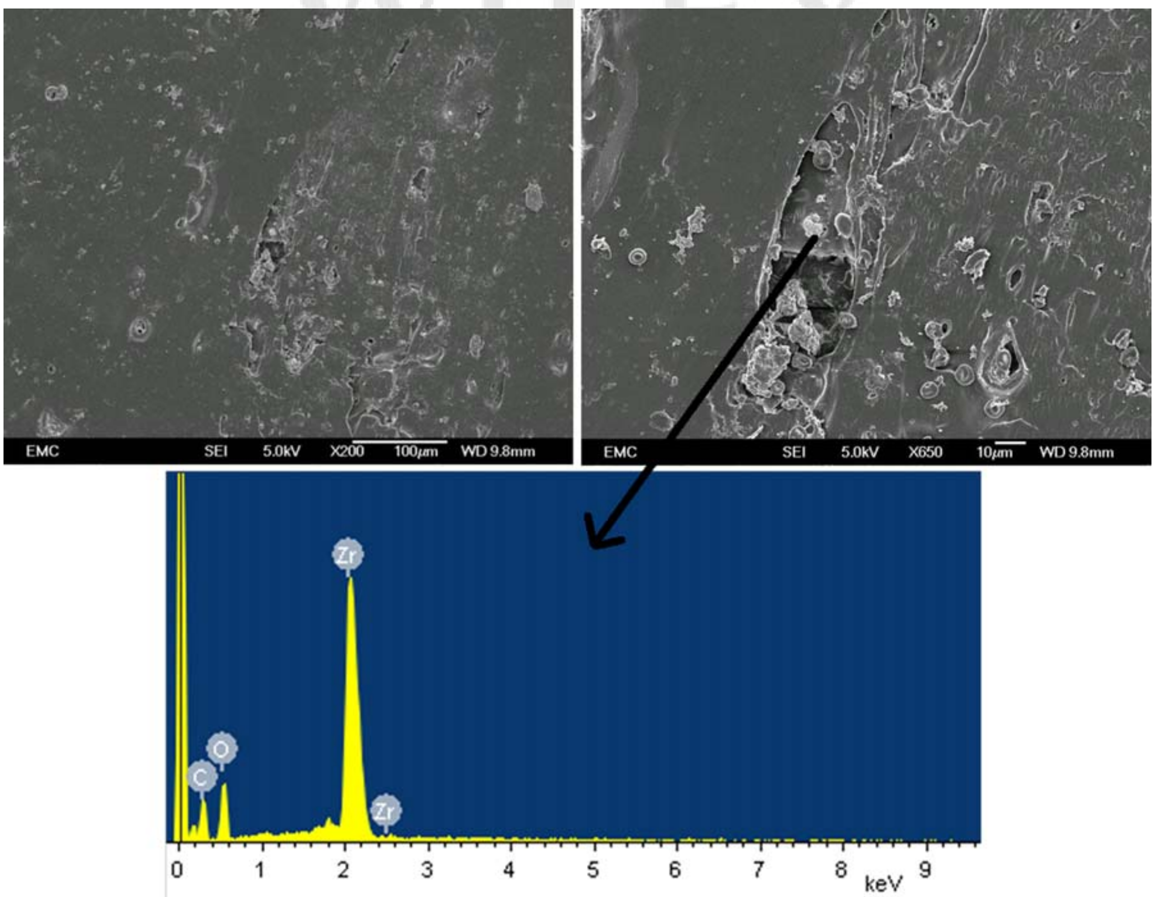

COLOR

FIGURE 4. SEM and EDX demonstrating the presence of zirconium dioxide particles within the surface voids of the undamaged regions of the cement

COLOR

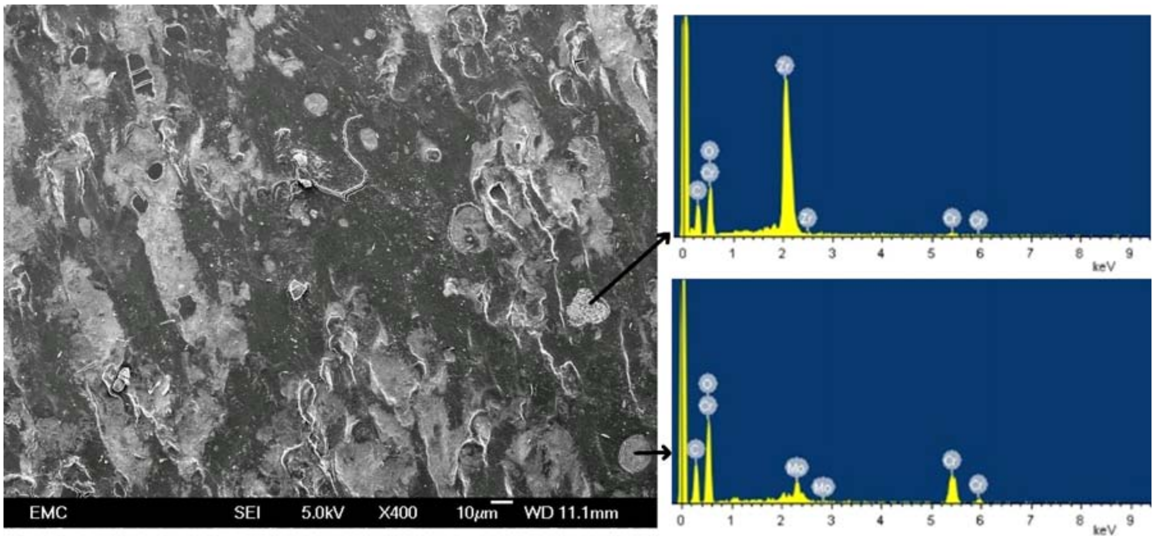

FIGURE 5. SEM and EDX of the moderately damaged cement surface showing deformation of the cement and the presence of ZrO_2 particles and transferred Cr and Mo.

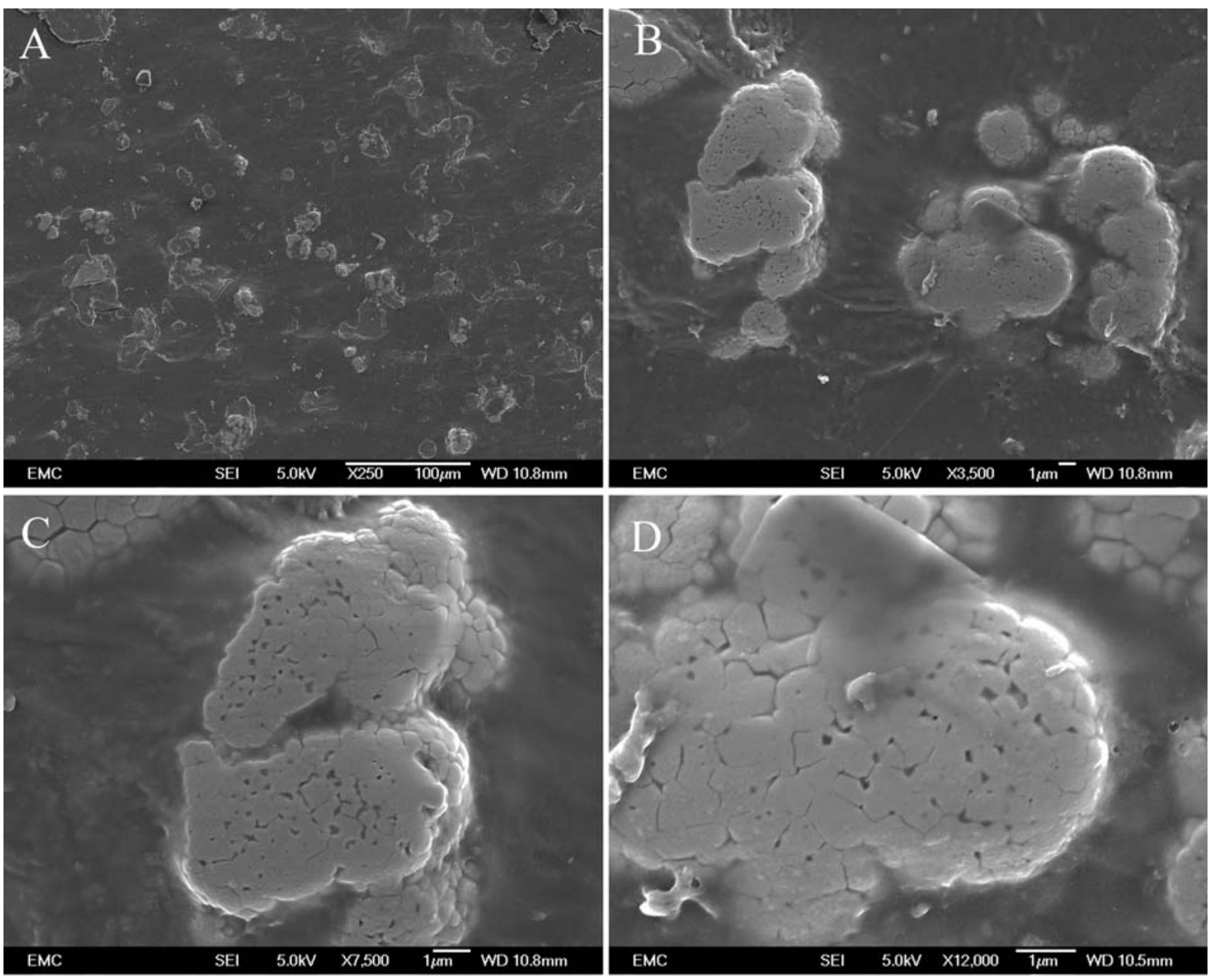

FIGURE 6. SEM micrographs the cement surface from a highly damaged stem, showing the ZrO_2 particles protruding from the surface of the cement. Images are increasing magnification of the same particle (A) 250× magnification, (B) 3500× magnification, (C) 7500× magnification, and (D) 12,500× magnification.

TABLE II.IC. P-MS Results from the Corrosion Product of Stem 8

Element	Cr	Co	Zr	Mn	Fe	W	Mo
Concentration (ppm)	114,000	11,700	142	103	97.2	17.2	8.5

on the corresponding femoral stem components. The location and morphology of the damage to the femoral stem components in this study is in keeping with that of previous retrieval work. The major regions of material loss were on the posterior and medial sides of the implants, with directionality to the deformation within Gruen zones 1 and 7 in agreement with the findings of previous studies.[2–4] The directionality in the damage is a reflection of the motion and peak loading between the cement and the stem *in vivo*[20] and provides evidence for the tribocorrosive damage having a primarily mechanical origin.

Examination of the retrieved cement surfaces has highlighted that the radiopacifier may have a more detrimental role than previously hypothesized in the damage seen at the proximal end of the cement-stem overlap. Howell et al.[3] found no significant difference between the presence of radiopacifier in the cement and the stem wear score, although the number of stems with radiolucent cement in the study was comparatively small. Zhang et al.[17] did a comparative study between three different cements (Simplex P, Palacos R and CMW 3) and demonstrated no significant difference in the stem surface damage generated by the different cements. The study attributed the damage to their previous hypothesis[13,17,21–24] that it was the pores at the interface which initiated the damage. However, the EDX traces of voids demonstrated the presence of radiopacifier particles as observed in this study, but it was not commented upon by the authors.[17] The study also hand mixed the cement in a bowl, which is likely to have introduced a higher density of voids compared to the standard vacuum mixing method used clinically to produce the cement reviewed in this study. These observations were used as a justification by Bryant et al.[4,11] to rule out the radiopacifier as having an abrasive effect.

The undamaged regions of the cement within this study revealed voids at the stem cement interface. The origins of these voids are not clear, but as the cement was vaccum mixed, they are likely due to shrinkage during the curing of the cement after insertion. Investigations of the surface voids in this study showed the presence of radiopacifier particles in the voids and in close proximity to the surface. However, there was no damage on the stems of this study that matched the reported damage patterns presented by Zhang et al.[13,17,21–24] and Blunt et al.[25]

The cement from the areas of high stem surface damage had rough surfaces with zirconium dioxide radiopacifier agglomerates not only protruding from the surface but also worn flat. The hard, abrasive radiopacifier agglomerates would have been in direct contact with the stem surface and would have had the ability to plough and plastically deform the stem surface, disrupting the passive oxide film and repassivation process, increasing the susceptibility to corrosive attack.

The ICP-MS analysis of the corrosion product in this study showed the presence of a range of ions, with the majority of trace elements from the CoCrMo alloy of the stem. The ICP-MS analysis results show that the make-up of the film was 90.3% Cr, 9.3% Co, 0.11% Zr, and 0.007% Mo with the rest of the elements making up the difference. The result implies that the film is Cr rich, with evidence of the radiopacifier within the film. These findings are consistent with the compacted Cr_2O_3 film seen in the analysis performed by Bryant et al.[15] The detailed compositional analysis conducted in their study only considered the metallic species associated with the stem alloy and signs of protein and did not look for evidence of the barium sulphate radiopacifier within the film. However, their earlier work[11,12] highlighted that the cement chemistry, particularly sulfates from the $BaSO_4$ radiopacifier, can enhance corrosion of the stem surface. The disparity between the level of Co in the film compared to the 60–70% cobalt content of the stem alloy is linked to the thermodynamic stability of the species within the cement stem interface. The study by Lewis et al.[24] investigated the effects of different fluids on the dissolution and corrosion of CoCrMo alloys. The study provided values of the Gibb's free energy (ΔG°) for the formation of Cr_2O_3, $Cr(OH)_3$, and CoO as -1058, -984, and -214 kJ mol^{-1}, respectively. The more negative the ΔG° the more thermodynamically favorable the reaction, and hence the chromium remains in the interface, reforming the oxide film, while the Co ions are removed in solution. The study also reviewed the effects of proteins on the corrosion by looking at the first equilibrium constants (K) for the polydentate ligand EDTA, and the values for Co and Cr were $K_{Cr} = 2.5 \times 10^{23}$ and $K_{Co} = 1.2 \times 10^{16}$, indicating that Cr ions are more likely to complex with proteins than Co. This was demonstrated experimentally by Clark and Williams[25] using metal powders; the presence of protein increased the corrosion rate of cobalt and chromium by 30–40 times and 2–4 times, respectively, with the metals forming protein–metal complexes. AQ4

On the basis of the present work, a new mechanism is proposed for the proximal surface damage. After implantation the stem sits within a close fitting cement mantle. The initial loading of the implant results in the stem sinking into the cement mantle and the formation of hoop stresses which hold the stem in the mantle. This initial sinking can range from 0.32 to 1.2 mm over 2 years depending on the stem design.[26] The surface finish of the stems is polished, but there is a roughness (Ra) of 0.1 μm and between the sinking in and the millions of loading cycles resulting in micromotion at the interface, the 0.1 μm CoCrMo asperities on the stem wear and deform the PMMA cement surface. This process results in the subsurface radiopacifier agglomerates within the cement reaching the surface and forming asperities similar to those observed on the retrieved cement surfaces in this study. These asperities are harder (12–13 GPa) than the CoCrMo surface (6.0 GPa), and the subsequent cyclical micromotion results in regular depassivation and deformation of the stem surface.

CONCLUSION

This study investigated the surface of retrieved bone cement in relation to the damage seen on matched retrieved stems. The retrieved cement surfaces all showed evidence of radiopacifier agglomerates protruding from or at the surface, which was in contact to the stem. The ICP-MS results indicate that a tribocorrosive mechanism was the cause of the damage to the stems; however, the depassivation and plastic deformation of the stem surface is attributable to micromotion between the radiopacifier agglomerates and the stem surface.

CONFLICT OF INTERESTS

Jeremy Latham is a consultant for Zimmer, DePuy, and Lima LTO. Richard Cook has undertaken paid consultancy for Biomet.

REFERENCES

1. Willert HG, Broback LG, Buchhorn GH, Jensen PH, Koster G, Lang I, Ochsner P, Schenk R. Crevice corrosion of cemented titanium alloy stems in total hip replacements. Clin Orthop Relat Res 1996; 333:51–75.
2. Donell ST, Darrah C, Nolan JF, Wimhurst J, Toms A, Barker TH, Case CP, Tucker JK, Norwich Metal-on-Metal Study Group. Early failure of the Ultima metal-on-metal total hip replacement in the presence of normal plain radiographs. J Bone Joint Surg Br 2010; 92(11):1501–1508.
3. Howell JR, Blunt LA, Doyle C, Hooper RM, Lee AJC, Ling RSM. In vivo surface wear mechanisms of femoral components of cemented total hip arthroplasties: The influence of wear mechanism on clinical outcome. J Arthroplasty 2004;19(1):88–101.
4. Bryant M, Ward M, Farrar R, Freeman R, Brummitt K, Nolan J, Neville A. Failure analysis of cemented metal-on-metal total hip replacements from a single centre cohort. Wear 2013;301(1–2):226–233.
5. Bolland BJ, Culliford DJ, Langton DJ, Millington JP, Arden NK, Latham JM. High failure rates with a large-diameter hybrid metal-on-metal total hip replacement: Clinical, radiological and retrieval analysis. J Bone Joint Surg Br 2011;93(5):608–615.
6. Thomas SR, Shukla D, Latham PD. Corrosion of cemented titanium femoral stems. J Bone Joint Surg Br 2004;86(7):974–978.
7. Ellison P, Hallan G, Høl PJ, Gjerdet NR, Havelin LI. Coordinating retrieval and register studies improves postmarket surveillance. Clin Orthop Relat Res 2012;470(11):2995–3002.
8. Grose A, González Della Valle A, Bullough P, Lyman S, Tomek I, Pellicci P. High failure rate of a modern, proximally roughened, cemented stem for total hip arthroplasty. Int Orthop 2006;30(4): 243–247.
9. Valle AGD, Rana A, Nestor B, Bostrom M, Westrich G, Salvati EA. Metallic shedding, surface finish changes, and extensive femoral osteolysis in the loose spectron EF stem. Clin Orthop Relat Res 2006;442:165–170.
10. Bryant M, Ward M, Farrar R, Freeman R, Brummitt K, Nolan J, Neville A. Characterisation of the surface topography, tomography and chemistry of fretting corrosion product found on retrieved polished femoral stems. J. Mech. Behav. Biomed. Mater 2013. AQ5
11. Bryant M, Farrar R, Freeman R, Brummitt K, Neville A. Fretting corrosion characteristics of polished collarless tapered stems in a simulated biological environment. Tribol Int 2013;65:105–112.
12. Jiang XQ, Blunt L, Barrans S, Brown L, Zhang HY. Investigation of relative micromotion at the stem–cement interface in total hip replacement. Proc Inst Mech Eng H: J Eng Med 2009;223(8): 955–964.
13. Zhang HY, Brown L, Blunt L, Jiang XQ, Barrans S. The contribution of the micropores in bone cement surface to generation of femoral stem wear in total hip replacement. Tribol Int 2011; 44(11):1476–1482.
14. Bryant M, Hu X, Farrar R, Brummitt K, Freeman R, Neville A. Crevice corrosion of biomedical alloys: A novel method of assessing the effects of bone cement and its chemistry. J Biomed Mater Res B: Appl Biomater 2013;101(5):792–803.
15. Bryant M, Farrar R, Brummitt K, Freeman R, Neville A. Fretting corrosion of fully cemented polished collarless tapered stems: The influence of PMMA bone cement. Wear 2013;301(1–2): 290–299.
16. Espehaug B, Furnes O, Havelin LI, Engesaeter LB, Vollset SE. The type of cement and failure of total hip replacements. J Bone Joint Surg Br 2002;84(6):832–838.
17. Zhang HY, Blunt LA, Jiang XQ, Fleming LT, Barrans SM. The influence of bone cement type on production of fretting wear on the femoral stem surface: A preliminary study. Clin Biomech 2012;27(7):666–672.
18. Bryant M, Ward M, Farrar R, Freeman R, Brummitt K, Nolan J, Neville A. Characterisation of the surface topography, tomography and chemistry of fretting corrosion product found on retrieved polished femoral stems. J Mech Behav Biomed Mater 2014;32:321–334.
19. Beake BD, Liskiewicz TW. Comparison of nano-fretting and nano-scratch tests on biomedical materials. Tribol Int 2013;63:123–131.
20. Kleemann RU, Heller MO, Stoeckle U, Taylor WR, Duda GN. THA loading arising from increased femoral anteversion and offset may lead to critical cement stresses. J Orthop Res 2003;21(5): 767–774.
21. Zhang H, Brown L, Blunt L, Barrans S. Generation of fretting wear debris at the stem-cement interface in total hip replacement. In: Lucas G, editor. Proceedings of the Computing and Engineering Annual Researchers' Conference 2007: CEARC'07. Huddersfield: University of Huddersfield; 2007. pp 1–4.
22. Zhang H, Brown L, Blunt L, Barrans S. Evaluation of fretting wear on the femoral stem surface. In: International Conference on Bioengineering and Biomaterials. Meknes, Morocco: ENSAM,; 2009.
23. Zhang H, Brown LT, Blunt LA, Jiang X, Barrans SM. Understanding initiation and propagation of fretting wear on the femoral stem in total hip replacement. Wear 2009;266(5–6):566–569.
24. Zhang HY, Blunt L, Jiang XQ, Brown L, Barrans S, Zhao Y. Femoral stem wear in cemented total hip replacement. Proc Inst Mech Eng H 2008;222(5):583–592.
25. Blunt LA, Zhang H, Barrans SM, Jiang X, Brown LT. What results in fretting wear on polished femoral stems. Tribol Int 2009;42(11–12):1605–1614.
26. Alfaro-Adrián J, Gill HS, Murray DW. Cement migration after THR: A comparison of Charnley elite and Exeter femoral stems using RSA. J Bone Joint Surg Br 1999;81 (1):130–134.

AQ1: Please check the inserted running title for correctness or provide an alternate one with a maximum of ∼70 characters including spaces.

AQ2: Please provide the department details for affiliations 1–4.

AQ3: Please confirm whether the designated corresponding author is correct.

AQ4: The author names “Lewis et al.” and “Clark and Williams” given along with the citation of Refs. 24 and 25 do not match with that of the reference list. Please check.

AQ5: Please update Ref. 10.

AQ6: Please confirm that given names (red) and surnames/family names (green) have been identified correctly.

Please confirm that the funding sponsor list below was correctly extracted from your article: that it includes all funders and that the text has been matched to the correct FundRef Registry organization names. If a name was not found in the FundRef registry, it may be not the canonical name form or it may be a program name rather than an organization name or it may be an organization not yet included in FundRef Registry. If you know of another name form or a parent organization name for a not found item on this list below, please share that information.

FundRef name	**FundRef Organization Name (Country)**	**FundRef DOI**	**Grant IDs**
EPSRC through the Green Tribology Platform grant (Natalie Shearwood-Porter)	Engineering and Physical Sciences Research Council	10.13039/501100000266	EP/J001023/1